Field-free molecular orientation induced by single-cycle THz pulses: the role of resonance and quantum interference

Shu, Chuan-Cun; Henriksen, Niels Engholm

Published in:
Physical Review A

Link to article, DOI:
10.1103/PhysRevA.87.013408

Publication date:
2013

Document Version
Publisher's PDF, also known as Version of record

Field-free molecular orientation induced by single-cycle THz pulses: The role of resonance and quantum interference

Chuan-Cun Shu and Niels E. Henriksen*

Department of Chemistry, Technical University of Denmark, Building 207, DK-2800 Kgs. Lyngby, Denmark

(Received 14 September 2012; published 7 January 2013)

We consider the rotational excitation of molecules induced by asymmetric ("half-cycle") as well as symmetric single-cycle THz pulses, leading to field-free time-dependent orientation. We show that the basic excitation mechanisms are very similar for the two types of pulses; i.e., the frequency distributions of the pulses at the rotational resonance frequencies play an important role. Furthermore, we investigate the interference between multiple rotational excitation pathways following prealignment with a nonresonant 800-nm femtosecond pulse. It is shown that such interference can lead to an enhancement of the orientation of the linear HCN molecule by a factor close to 2.

DOI: 10.1103/PhysRevA.87.013408 PACS number(s): 33.80.−b, 37.10.Vz, 32.80.Qk, 42.50.Hz

I. INTRODUCTION

The angular distribution of molecules plays an important role for the outcome of molecular collisions as well as for the interaction between molecules and electromagnetic radiation. One can restrict this angular distribution in various ways. For example, perfect alignment implies that a molecular axis is completely parallel to a space-fixed axis, e.g., defined by a field polarization vector. Perfect orientation implies not only perfect alignment but, in addition, that an oriented molecular axis (consider a diatomic AB molecule as a simple example) is in the same direction as a chosen oriented space-fixed axis. Thus, orientation implies the breaking of inversion symmetry. For recent experimental demonstrations of laser-induced alignment, see [1,2] and references therein. Laser-induced orientation is less developed.

Orientation has been theoretically predicted [3] and experimentally demonstrated [4,5] by combining electrostatic fields and pulsed nonresonant laser fields. Methods based on pulsed two-color phase-locked laser fields have also been studied both theoretically and experimentally [6–8]. Aligned and oriented molecules have recently been considered in areas such as molecular frame photoelectron angular distributions [9–11], molecular imaging [12,13], and high-order harmonic generation [14,15].

Some time ago, it was suggested that field-free orientation of molecules can be created after the interaction with a short THz pulse [16–18]. Thus, after the irradiation, highly oriented states appear periodically. The basic mechanism is based on the creation of a rotational wave packet which consists of a superposition of rotational states with even and odd angular momentum quantum numbers J. The physical basis for the orientation is the interference between even and odd J states which have different parities with respect to inversion at the origin [16,17].

Asymmetric "half-cycle" pulses (HCPs), with a strong amplitude asymmetry between the positive and the negative parts of the electric field [16–18], as well as nearly symmetric single-cycle THz pulses [19] have been considered in this context. In addition, there are several theoretical works which have elaborated on these ideas; see, e.g., [20–22] and references therein. Recently, the first experimental demonstration was published [23]. Compared with the methods already in use, the very intense laser fields of the approach using two-color phase-locked fields are avoided, and an advantage of the pulsed THz-induced orientation compared with the method based on electrostatic fields is the field-free nature of the orientation.

In a recent theoretical study [24], the excitation mechanism related to intense nearly single-cycle THz pulses was analyzed. It was concluded that molecules are resonantly excited by the THz pulse because the energy spacings between neighboring rotational states are comparable to the frequency components of the THz pulse [24]. In addition, it was suggested that this mechanism differs from that of the HCP interaction, in which, according to previous descriptions [16–18], the interaction has been described as an angular momentum kick. In this work we will consider this question in more detail by investigating the role of resonance for HCPs as well as symmetric single-cycle pulses.

Furthermore, it was demonstrated that an enhancement of the molecular orientation could be obtained after prealignment of the molecule [24] (see also [25,26] for a related scheme). Thus, pre-excitation with a nonresonant femtosecond (fs) laser pulse creates (via Raman-type transitions) a superposition of rotational states with either only even J or only odd J values. Subsequent interaction with a THz pulse leads then to orientation. The role of the pre-excitation is to open new transitions with transition frequencies which might be resonant with the subsequent THz pulse [24] and, in addition, to allow for quantum interference between multiple excitation pathways. We disentangle here the two mechanisms in order to quantify the role of quantum interference.

In this work we investigate the above-mentioned questions by elaborating on a previously developed analytical description [16] as well as by numerical calculations on the linear HCN molecule. The initial state is assumed to be a pure rotational eigenstate.

II. MOMENTUM KICK AND RESONANCE

We consider a molecule subjected to a flash of electromagnetic THz radiation. The field-free Hamiltonian for a linear

*neh@kemi.dtu.dk

rigid rotor is

$$\hat{H}_0 = \frac{\hbar^2 \hat{J}^2}{2I} = B\hat{J}^2, \tag{1}$$

where I is the moment of inertia and $\hat{J}^2$ is the (dimensionless) squared angular momentum operator. We have introduced the rotational constant $B = \hbar^2/(2I)$, here defined in the unit of energy [the rotational constant is also often defined in the unit of frequency, i.e, as $B/h = \hbar/(4\pi I)$]. The coupling term with the electric field $\mathbf{E}(t)$ takes, within the electric dipole approximation for a linearly polarized field, the form

$$V_{\rm int}(t) = -\boldsymbol{\mu}\cdot\mathbf{E}(t) = -\mu E_0 a(t)\cos(\omega t)\cos\theta, \tag{2}$$

where μ is the permanent dipole moment, θ is the polar angle between the molecular axis and the polarization direction of the laser field, E_0 is the maximum field amplitude, $a(t)$ is the envelope of the field peaked around $t = 0$ and nonzero for $t \in [t_i, t_f]$, and ω is the carrier frequency of the field.

In the sudden- or impulsive-impact limit, the time-evolution operator can be represented by the first term in the Magnus expansion, which is superior to low-order perturbation theory in the impulsive limit [16]. The dynamics of the rotational wave packet with the rotational eigenstate $Y_{\rm JM}(\theta,\phi)$ as the initial state is then given by [16] (neglecting the part of the time-evolution operator which generates rotations during the pulse)

$$|\Psi(\theta,\phi,t)|^2 = |\hat{U}_0(t,0)e^{i(A/\hbar)\cos\theta}Y_{\rm JM}(\theta,\phi)|^2, \tag{3}$$

where the time t is longer than the pulse duration, $\hat{U}_0(t,0) = \exp[-i\hat{H}_0 t/\hbar]$ is the time-evolution operator for free rotational dynamics, and A is given by

$$A = \mu E_0\{F_0(\omega) + i(\hbar/I)F_1(\omega) + \cdots\}, \tag{4}$$

where

$$F_n(\omega) = \int_{t_i}^{t_f} t^n a(t)\cos(\omega t)dt \tag{5}$$

for $n = 0,1,\ldots$. The first few terms in Eq. (4) suffice when the pulse is short on the time scale of rotational motion. We note that

$$F_0(\omega) = (1/E_0)\int_{t_i}^{t_f} E(t)dt = 0, \tag{6}$$

since the time integral over the electric field is 0.

However, for an ultrashort asymmetric HCP, the effect of the long weak negative tail can be neglected, and integration restricted to the strong unipolar part gives effectively $F_0(\omega) \neq 0$, whereas $F_1(\omega) = 0$ [16]. This result is exactly as in [18], in which, subsequently, only the envelope (i.e., no carrier frequency, $\omega = 0$) was used to represent the field. In [18], it was shown that this approximation works well for a HCP. Note that, in this limit, there is no explicit dependence of A [see Eq. (4)] on the resonance frequencies for rotational transitions, e.g., $\omega_{\rm rot} = \hbar/I$ ($\omega_{\rm rot} = 2\pi\nu_{\rm rot}$, where $\nu_{\rm rot} = 2B/h$). The "pulse operator" $\exp[i(A/\hbar)\cos\theta]$ in Eq. (3) creates a superposition of rotational states, with the selection rule $\Delta M = 0$ [16]. Thus, the action of this operator can be described as an angular momentum boost or kick for a rotationless ($J = 0$) initial state.

At this point it is useful to make a comparison with the result obtained within first-order perturbation theory [27]. Here the amplitude for a transition from state s to state k is proportional to the Fourier transform of the electric field $E(t)$ at the transition frequency $\omega = \omega_{ks}$. That is, for an ultrashort pulse where the Fourier transform basically is constant, there is no dependence on the resonance frequency because the frequency distribution is broad enough to provide, essentially, constant field components at frequencies that induce transitions. This is in agreement with the result discussed above.

For a nearly symmetric single-cycle THz pulse, $F_0(\omega) = 0$, whereas $F_1(\omega) \neq 0$. A in Eq. (4) depends now on $\omega_{\rm rot} = \hbar/I$ and is proportional to the Fourier transform of $E(t)$ at $\omega_{\rm rot}$, which can be written in the form $\{F_0(\omega) + i(\hbar/I)F_1(\omega) + \cdots\}$ for a short pulse. Furthermore, in the weak-interaction limit ($A/\hbar \to 0$) the well-known selection rule $\Delta J = \pm 1$ is also fulfilled, and, with the rotational ground state as the initial state, it is easy to show [16] that Eq. (3) coincides with the result obtained within first-order perturbation theory. Note, however, that the transition probabilities to be considered in the following are substantially larger than what can be predicted by first-order perturbation theory (the population depletion of the initial state is, e.g., substantially larger than a few percent).

In previous works, more elaborate and, in part, alternative discussions of the relevant analytical descriptions and mechanisms have been presented [19,28], but the discussion above suggests that the excitation mechanism for a HCP or a symmetric single-cycle pulse can be understood within the same description.

III. NUMERICAL ILLUSTRATION

Via numerical calculations, we further investigate the role of resonance as well as quantum interference effects. The setup, as used in [24], is shown in Fig. 1(a). The HCN molecule, in its ground state, taken as a linear rigid rotor, offers an illustrative example, in a model describing both permanent dipole moment μ and polarizability $\alpha_\parallel$ and $\alpha_\perp$ (parallel and perpendicular components) interactions. The complete molecule-plus-field Hamiltonian, at that level of approximation, is [29]

$$\hat{H}(t) = B\hat{J}^2 - \mu\mathcal{E}(t)\cos\theta - \frac{\mathcal{E}^2(t)}{2}(\Delta\alpha\cos^2\theta + \alpha_\perp), \tag{7}$$

where $\mathcal{E}(t)$ is the total electric field of a nonresonant femtosecond pulse and a time delayed THz pulse and $\Delta\alpha = \alpha_\parallel - \alpha_\perp$ is the polarizability anisotropy. All relevant parameters are taken from [30]. We note that the permanent dipole moment is $\mu = 2.89$ D and the rotational constant is $B/h = 0.0437$ THz or, in wave numbers, $\tilde{B} = 1.457$ cm^{-1}. The time evolution of the wave packet $\Psi(\theta,t)$, starting from a rotational eigenstate of the electronic ground state, is governed by the time-dependent Schrödinger equation [17,31], which is numerically solved by the split-operator method. We employ the expectation value of $\cos\theta$, $\langle\cos\theta\rangle(t) = \langle\Psi(\theta,t)|\cos\theta|\Psi(\theta,t)\rangle$, to measure the degree of orientation, with $\langle\cos\theta\rangle(t) \in [-1,1]$.

We use in the calculations a nonresonant 800-nm laser with the peak intensity of 2.0×10^{13} W/cm^2 and the pulse duration 100 fs (full width at half maximum in intensity) in order to prealign the molecule. A nearly symmetric single-cycle THz pulse with the peak electric-field amplitude of 1.0×10^7 V/m

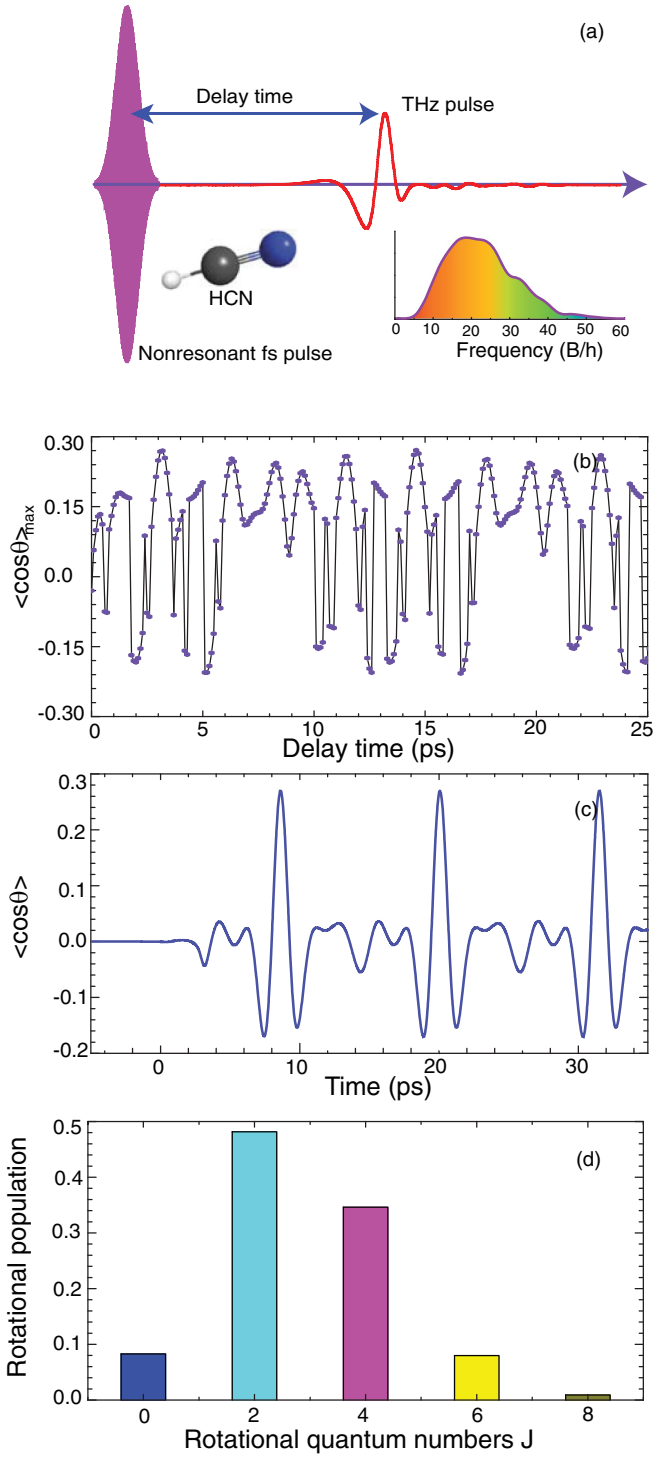

FIG. 1. (Color online) (a) Schematic illustration of the visible fs and THz laser pulses, where the delay time is the time shift between the centers of the two pulses. The frequency distribution of the THz pulse is also shown in units of the rotational constant B of HCN. (b) The maximum of $\langle \cos\theta \rangle$ as a function of delay time. (c) The degree of field-free orientation $\langle \cos\theta \rangle$ as a function of time (at delay time 3.2 ps). (d) The rotational state distribution after the interaction with the visible fs laser pulse.

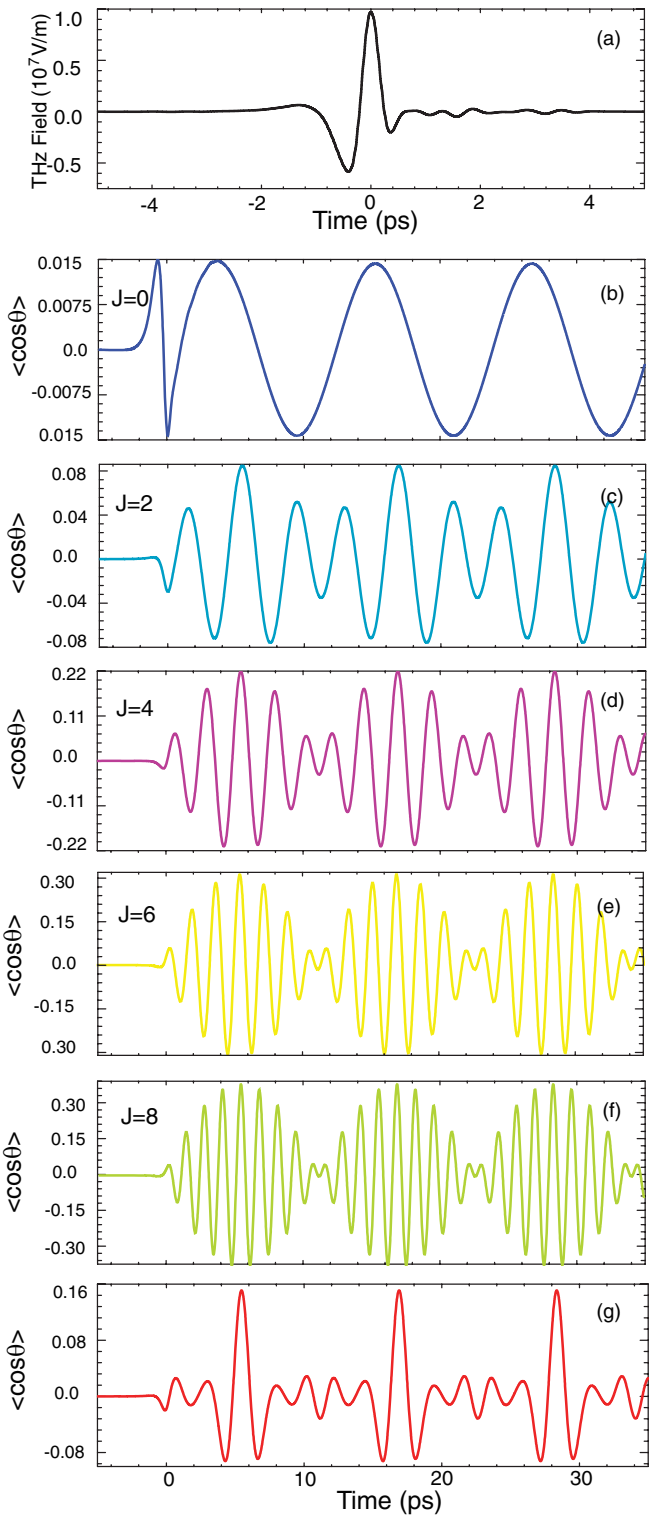

FIG. 2. (Color online) The degree of field-free orientation $\langle \cos\theta \rangle$, as a function of the initial rotational quantum number J, induced by the single-cycle THz pulse in the top panel. The lowest panel shows the overall orientation after the THz pulse as an incoherent (classical) average over the rotational distribution in Fig. 1(d).

and a central frequency around 1.0 THz is also shown in Fig. 1(a). Such a THz pulse can be created experimentally (see, e.g., [32]).

For the nearly symmetric single-cycle case, results are shown in Figs. 1 and 2. Figure 1(b) shows the maximum orientation $\langle \cos\theta \rangle(t)$ obtained for various fixed delay times

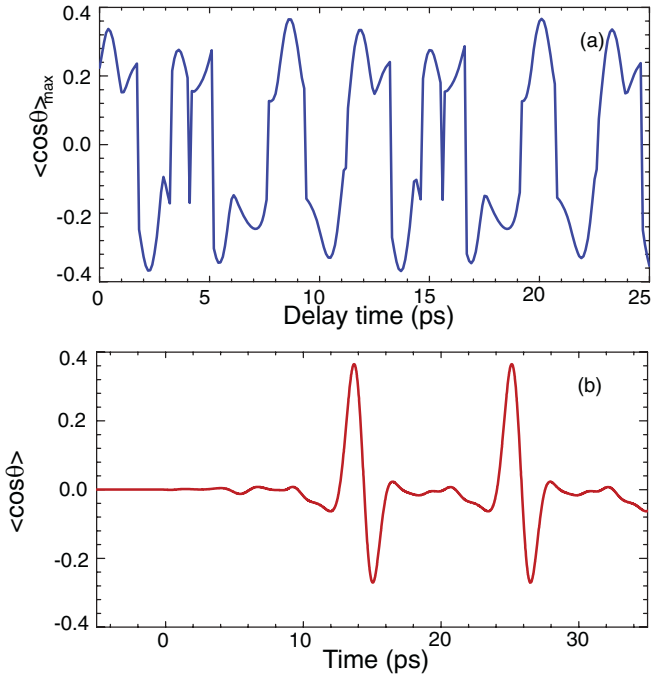

FIG. 3. (Color online) Same as Figs. 1(b) and 1(c) but now for the half-cycle pulse shown in Fig. 4. (a) The maximum of $\langle \cos\theta \rangle$ as a function of delay time [as in Fig. 1(b), the apparent erratic behavior at some delay times is due to the sparseness of the calculated delay points]. (b) The degree of field-free orientation $\langle \cos\theta \rangle$ as a function of time (at delay time 8.7 ps).

(marked by the dots; the line is drawn to guide the eye) between the 800-nm nonresonant laser pulse and the THz pulse. The maximum numerical value including sign is given; that is, for some delay times the maximum orientation corresponds to preferred orientation into the forward hemisphere, and for other delay times the largest degree of orientation is into the backward hemisphere. We observe clearly from Fig. 1(c) that after the irradiation, that is, for times larger than about 1 ps, oriented molecular states appear in a periodic fashion. Figure 1(d) shows the population of the rotational states after the alignment and prior to the interaction with the THz pulse.

Figure 2 shows the degree of field-free orientation as a function of the initial rotational quantum number J. When Figs. 1(c) and 2 ($J = 0$) are compared, significant enhancement of the orientation is observed due to prealignment. At the field strength considered in this work, the transitions induced by the THz pulse obey to good accuracy the selection rule $\Delta J = \pm 1$. Thus, the (one-photon) transition and resonance frequencies for the transitions $J \rightarrow J + 1$ are $2B(J + 1)/h$, and for the transitions $J \rightarrow J - 1$ they are $2BJ/h$. We observe from Fig. 2 that the orientation obtained for the initial rotational quantum numbers $J = 0$ and 2 is very modest, whereas the orientation obtained for $J = 4$,6, and 8 is much higher. This correlates well with the transition frequencies and the frequency distribution (the absolute square of Fourier transform) of the THz pulse shown in Fig. 1. We note in passing that it is possible experimentally to select individual rotational eigenstates from a thermal distribution of rotational states [5,33,34].

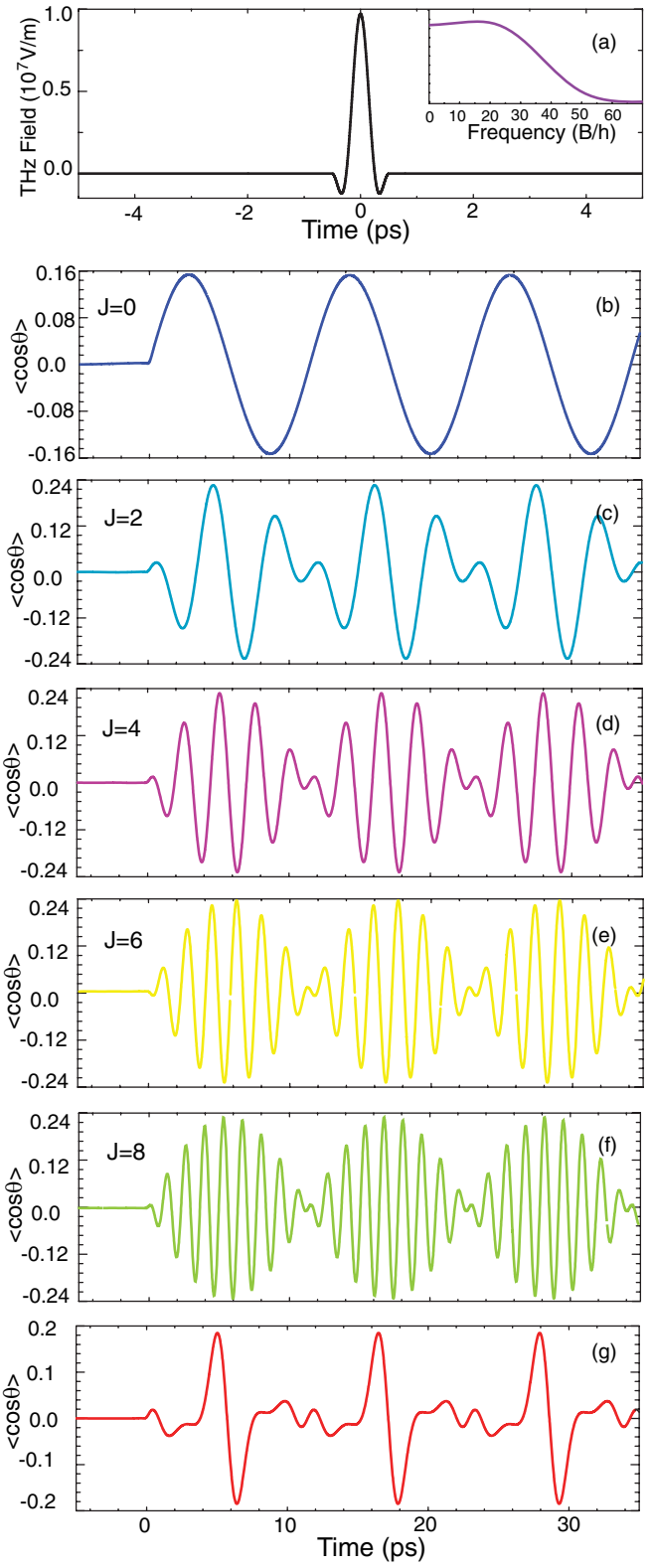

FIG. 4. (Color online) The degree of field-free orientation $\langle \cos\theta \rangle$, as a function of the initial rotational quantum number J, induced by the half-cycle THz pulse in the top panel. Inset: frequency distribution of the pulse in units of the rotational constant B of HCN. The lowest panel shows the overall orientation after the THz pulse as an incoherent (classical) average over the rotational distribution in Fig. 1(d).

Clearly, the prealignment of the molecule corresponding to the creation of population in the states $J = 2,4,6,\ldots$ opens new transitions, which give better resonance conditions due to larger frequency components of the THz pulse at the relevant resonance frequencies [24]. Thus, the rather high degree of HCN orientation obtained even with a moderate field amplitude (1.0×10^7 V/m) is related to the favorable resonance conditions for transitions out of excited rotational states.

Furthermore, the time delay between the two pulses plays a role as shown in Fig. 1(b). This is a signature of coherent excitation and quantum interference [24,25]. The aligned molecule consists of a coherent superposition of rotational states [$J = 0,2,4,6,\ldots$, see Fig. 1(d)] with time-dependent phase factors. The final orientation depends also on the interference between these states induced by the THz pulse. Thus, population in the $J = 1$ state can be obtained via two different pathways: $J = 0 \rightarrow J = 1$ and $J = 2 \rightarrow J = 1$. Similarly, population in the $J = 3$ state can be obtained via two different pathways: $J = 2 \rightarrow J = 3$ and $J = 4 \rightarrow J = 3$. The importance of quantum interference between such pairs of pathways is analyzed by calculating an incoherent (classical) average of the orientation over the rotational distribution in Fig. 1(d). When we make a comparison with the result in Fig. 1(c), we deduce that the orientation can be enhanced by a factor close to 2 due to quantum interference.

Figures 3 and 4 show the results for a HCP represented by

$$E(t) = E_0 \sin^2\left[\frac{\omega(t + 0.5\tau)}{2N}\right]\cos(\omega t), \tag{8}$$

where the number of optical cycles $N = 1$, $\omega = 33$ cm^{-1} (1 THz), $\tau = 2N\pi/\omega$, and $E_0 = 1.0 \times 10^7$ V/m (the long duration weak and negative component of the HCP has negligible effects [18] and is not included). From Fig. 4, we note that the orientations obtained for all the initial J quantum numbers considered are very similar. This correlates well with the frequency distribution of the HCP shown in the top panel of Fig. 4. Again, when we compare the incoherent (classical) average with the result in Fig. 3(b), we deduce that the orientation can be enhanced by a factor close to 2 due to quantum interference.

IV. CONCLUSIONS

To conclude, we have discussed the "momentum kick mechanism" [16,18,30] and the "resonance mechanism" [24] for rotational excitation. For asymmetric as well as symmetric single-cycle THz pulses both mechanisms play a role. Thus, the creation of excited angular momentum states depends on the frequency distribution of the pulses and the resonance conditions. This is shown by numerical simulations, and it is predicted by the analytical Magnus expansion approach for impulsive excitation (in agreement with first-order perturbation theory in the weak-interaction limit). For the asymmetric HCPs, the orientation depends to a good approximation only on the integrated electric field (with the long negative tail dropped). Thus, no explicit dependence on the frequency distribution is observed, because the frequency distribution is broad enough to provide, essentially, constant field components at frequencies that induce rotational transitions. Finally, the role of quantum interference between multiple excitation pathways has been quantified.

ACKNOWLEDGMENTS

The Technical University of Denmark is acknowledged for a scholarship under the H. C. Ørsted postdoctoral program.

[1] F. Rosca-Pruna and M. J. J. Vrakking, Phys. Rev. Lett. **87**, 153902 (2001).
[2] H. Stapelfeldt and T. Seideman, Rev. Mod. Phys. **75**, 543 (2003).
[3] L. Cai, J. Marango, and B. Friedrich, Phys. Rev. Lett. **86**, 775 (2001).
[4] A. Goban, S. Minemoto, and H. Sakai, Phys. Rev. Lett. **101**, 013001 (2008).
[5] L. Holmegaard, J. H. Nielsen, I. Nevo, H. Stapelfeldt, F. Filsinger, J. Kupper, and G. Meijer, Phys. Rev. Lett. **102**, 023001 (2009).
[6] M. J. J. Vrakking and S. Stolte, Chem. Phys. Lett. **271**, 209 (1997).
[7] C. M. Dion *et al.*, Chem. Phys. Lett. **302**, 215 (1999).
[8] S. De *et al.*, Phys. Rev. Lett. **103**, 153002 (2009).
[9] L. Holmegaard *et al.*, Nat. Phys. **6**, 428 (2010).
[10] J. L. Hansen *et al.*, Phys. Rev. A **83**, 023406 (2011).
[11] J. L. Hansen, H. Stapelfeldt, D. Dimitrovski, M. Abu-samha, C. P. J. Martiny, and L. B. Madsen, Phys. Rev. Lett. **106**, 073001 (2011).
[12] C. Z. Bisgaard *et al.*, Science **323**, 1464 (2009).
[13] P. Hockett, C. Z. Bisgaard, O. J. Clarkin, and A. Stolow, Nat. Phys. **7**, 612 (2011).
[14] J. Itatani *et al.*, Nature (London) **432**, 867 (2004).
[15] T. Kanai, S. Minemoto, and H. Sakai, Nature (London) **435**, 470 (2005).
[16] N. E. Henriksen, Chem. Phys. Lett. **312**, 196 (1999).
[17] M. Machholm and N. E. Henriksen, Phys. Rev. Lett. **87**, 193001 (2001).
[18] C. M. Dion, A. Keller, and O. Atabek, Eur. Phys. J. D **14**, 249 (2001).
[19] D. Sugny, A. Keller, O. Atabek, D. Daems, S. Guérin, and H. R. Jauslin, Phys. Rev. A **69**, 043407 (2004).
[20] J. Salomon, C. M. Dion, and G. Turinici, J. Chem. Phys. **123**, 144310 (2005).
[21] C.-C. Shu, K.-J. Yuan, W.-H. Hu, and S.-L. Cong, Phys. Rev. A **80**, 011401(R) (2009).
[22] M. Lapert and D. Sugny, Phys. Rev. A **85**, 063418 (2012).
[23] S. Fleischer, Y. Zhou, R. W. Field, and K. A. Nelson, Phys. Rev. Lett. **107**, 163603 (2011).
[24] K. Kitano, N. Ishii, and J. Itatani, Phys. Rev. A **84**, 053408 (2011).
[25] E. Gershnabel, I. Sh. Averbukh, and R. J. Gordon, Phys. Rev. A **73**, 061401 (2006).
[26] E. Gershnabel, I. Sh. Averbukh, and R. J. Gordon, Phys. Rev. A **74**, 053414 (2006).

[27] E. Merzbacher, *Quantum Mechanics*, 2nd ed. (Wiley, New York, 1970).
[28] J. Ortigoso, J. Chem. Phys. **137**, 044303 (2012).
[29] N. Moiseyev and T. Seideman, J. Phys. B **39**, L211 (2006).
[30] C. M. Dion, A. B. Haj-Yedder, E. Cancés, C. LeBris, A. Keller, and O. Atabek, Phys. Rev. A **65**, 063408 (2002).
[31] C.-C. Shu, K.-J. Yuan, W.-H. Hu, and S.-L. Cong, J. Chem. Phys. **132**, 244311 (2010).
[32] P. U. Jepsen, D. G. Cooke, and M. Koch, Laser Photon. Rev. **5**, 124 (2011).
[33] R. B. Bernstein, *Chemical Dynamics via Molecular Beam and Laser Techniques* (Oxford University Press, New York, 1982).
[34] O. Ghafur *et al.*, Nat. Phys. **5**, 289 (2009).